

# All Sky Observations with BATSE and GBM

Colleen A. Wilson-Hodge<sup>1</sup> for the GBM and BATSE teams

<sup>1</sup> NASA/MSFC, Huntsville, AL 35812, USA  
*E-mail(CAWH): Colleen.Wilson@nasa.gov*

## ABSTRACT

The Burst and Transient Source Experiment (BATSE) on board the Compton Gamma Ray Observatory (CGRO) monitored the entire sky from 1991-2000. I will review highlights of BATSE observations including gamma ray bursts, black hole candidates, accreting pulsars, and active galaxies. On 2008 June 11, the Fermi Gamma Ray Space Telescope was launched. The Gamma ray Burst Monitor (GBM) on board Fermi continues the all-sky monitoring legacy started with BATSE. I will review early results and planned observations with GBM.

KEY WORDS: Fermi; GBM; Gamma Ray Bursts; X-ray binaries; Pulsars; Accretion; Earth occultation

## 1. Instrument Descriptions

### 1.1. BATSE

BATSE consisted of 8 detector modules positioned on the corners of the CGRO spacecraft. Each module consisted of two detectors, a large area detector (LAD) and a spectroscopy detector (SD), both of which were sodium iodide (NaI) scintillation crystals. Each LAD had a geometric area of 2025 cm<sup>2</sup>, a thickness of 1.27 cm, and was sensitive from about 25 keV to 1.8 MeV. Each SD had a geometric area of 126 cm<sup>2</sup>, a thickness of 7.62 cm, and depending on the gain settings, was sensitive from 8 keV - 10 MeV. The BATSE detectors viewed the entire unocculted sky at all times (Paciesas et al 1999).

### 1.2. GBM

GBM consists of 14 detector modules, 12 low-energy (8 keV-1 MeV) NaI detectors, and two high energy (150 keV- 30 MeV) bismuth germanate (BGO) detectors. Each NaI detector has a geometric area of 126 cm<sup>2</sup> and a thickness of 1.27 cm, while each BGO detector has a geometric area of 126 cm<sup>2</sup> and a thickness of 12.7 cm. The NaI detectors are arranged on the Fermi spacecraft to produce a 9 steradian field of view. Two detectors are positioned opposite each other looking 20 deg from the spacecraft zenith. Four detectors are evenly spaced around the spacecraft looking 45 deg from the spacecraft zenith. The remaining six detectors are evenly spaced around the spacecraft and are looking 90 deg from the spacecraft zenith. BGO detectors are positioned on the +X and -X sides of the spacecraft (Meegan et al 2007).

## 2704 BATSE Gamma-Ray Bursts

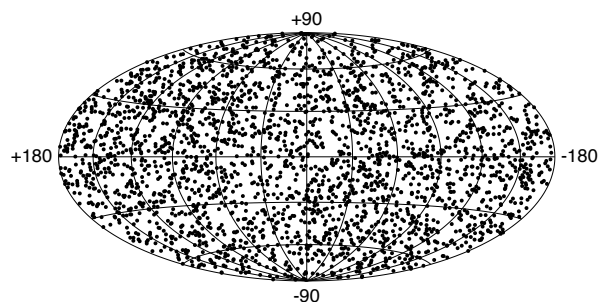


Fig. 1. The BATSE sky map, showing 2704 triggered gamma ray bursts over the 9 year mission, clearly illustrating the isotropy of gamma ray bursts.

## 2. Gamma Ray Burst Observations

### 2.1. BATSE

Before CGRO was launched, gamma ray bursts (GRBs) were believed to be galactic by many in the astronomical community. BATSE showed that these bursts had an isotropic angular distribution (Fig. 1), while the intensity distribution showed fewer weak bursts than expected from a homogeneous distribution of sources in Euclidean space. Because no observed galactic component had these spatial properties, BATSE provided the first clear indication that gamma ray bursts were of cosmological origin (Meegan et al. 1992).

BATSE triggered when it observed a change in count rate above a specified threshold (typically  $5.5 \sigma$ ) usually in the 50-300 keV band in either 64 ms, 256 ms, or 1.024 s timescales. In triggered mode, high rate data were accumulated for 573.4 s. During its 9 year mission, BATSE triggered a total of 8021 times. These

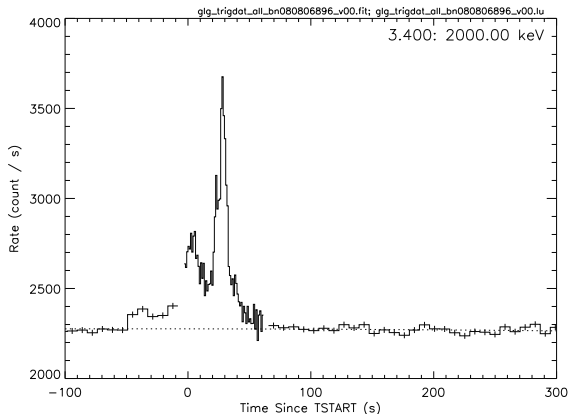


Fig. 2. The TRIGDAT light curve for a GRB observed with GBM on 2008 August 6 at 21:29:40 UT shows the combined count rates in all energy channels from GBM NaI detectors 1 and 2.

triggers included: 2704 GRBs, 1192 solar flares, 185 soft gamma repeaters, 2003 transient sources, 78 terrestrial gamma flashes, 1717 magnetospheric events, and 142 triggers that were phosphorescence spikes, accidental triggers, unknown events, or undetermined due to insufficient data (Paciesas et al. 1999, Briggs et al. in preparation).

## 2.2. GBM

GBM together with the Large Area Telescope (LAT) on-board Fermi will enable GRB observations over up to seven decades in energy. GBM continues the BATSE legacy and ties bursts observed with Fermi back to the well studied BATSE sample. GBM has 128 possible trigger algorithms, of which 62 are currently used. These algorithms contain combinations of energy bands and timescales from 16 ms - 4 s. Each trigger algorithm has an independently adjustable trigger threshold defined in terms of significance above background. GBM triggers when it detects a change in count rate above a specified threshold (typically  $4.5\text{--}5.5\sigma$ ) in at least two NaI detectors. Thereafter, it immediately alerts the TDRS satellites to send information about the trigger, called TRIGDAT, to the ground to facilitate observations with other observatories through GCN notices. This information includes the triggered detectors, triggered algorithm, on-board sky location, the on-board classification (e.g. GRB, Solar Flare, SGR, etc.), the flux, fluence, and significance of the trigger. In addition, an immediate signal is sent to the LAT along with a repoint recommendation if the burst fits pre-defined intensity and hardness criteria. During trigger mode, time tagged event data are produced for 300 seconds, the 8 channel continuous timing (CTIME) data are sped up from nominal 256 ms to 64 ms resolution, the 128 channel continuous spectra (CSPEC) are sped up from nominal 4.096 s to 1.024 s,

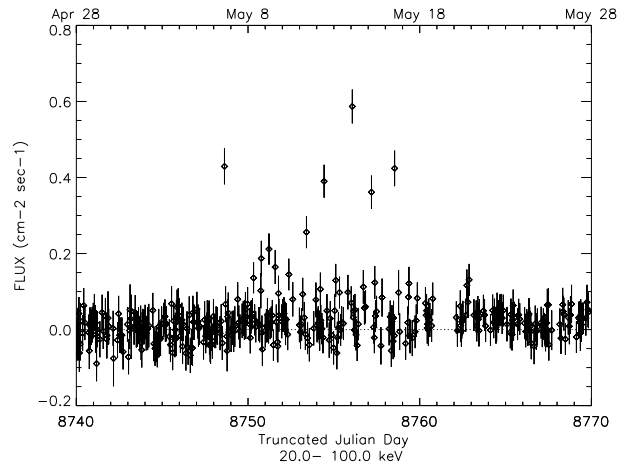


Fig. 3. From Paciesas et al. (1996). Single step Earth occultation measurements of GRS 1915+105 with BATSE in the 20-100 keV band during early May 1992. The high points on the plot are bright flares from GRS 1915+105 detected as large Earth occultation steps. For comparison, the flux from the Crab Nebula is  $\sim 0.3 \text{ ph cm}^{-2}\text{s}^{-1}$  in this band

and a ring buffer of 500,000 pre-trigger events is transmitted (Meegan et al 2007). An example TRIGDAT light curve from a burst observed with GBM in 2008 August is shown in Figure 2.

From 2008 July 13 (when triggers were enabled) until 2008 October 6, GBM triggered a total of 129 times. Of these triggers, 63 are identified as Gamma Ray Bursts, 33 as soft gamma repeaters or anomalous X-ray pulsars, four galactic X-ray binaries, and four terrestrial gamma flashes. The remaining 25 triggers are either too weak to identify, due to background fluctuations, or magnetospheric events.

## 3. Earth Occultation

The intensity of a galactic or extra-galactic source can be measured by calculating the difference in observed count rate before and after the source is occulted by the Earth. This measurement is most easily made using a small window of data surrounding the calculated time when the source of interest enters or exits Earth occultation. Projections of the Earth's limb on the sky at the time of these occultation "steps" can be used to locate new astrophysical sources. This technique is required for BATSE and GBM because neither instrument has direct imaging capabilities.

### 3.1. BATSE

With BATSE, we made extensive use of the Earth occultation technique. We monitored a catalog of 179 sources including primarily X-ray binaries, plus representative samples of active galaxies, X-ray emitting stars, and supernova remnants. From this catalog, we detected 74 X-ray binaries, three supernova remnants, and six active

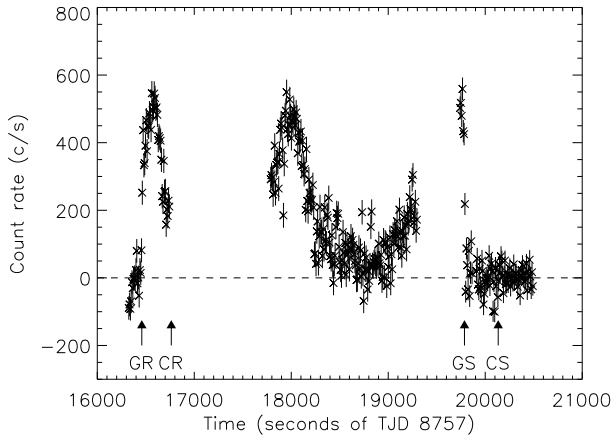


Fig. 4. From Paciasas et al. (1996). A flaring episode from GRS 1915+105 on 1992 May 15. Shown are background subtracted BATSE count rates with 8.192 s resolution in the 20-100 keV band summed over two detectors. GR, GS and CR, CS denote GRS 1915+105 and Cyg X-1 rise and set times, respectively. In this band, the Crab Nebula count rate is  $\sim 300 \text{ cts s}^{-1}$ .

galactic nuclei at  $10 \sigma$  or better either over the entire 9 year mission or in at least one identifiable outburst. Our limiting sensitivity was 3.5-20 mCrab, due to sky dependent systematic errors, over the 20-430 keV band (Harmon et al. 2004).

Although this technique is less sensitive than imaging instruments, it has the advantage of monitoring the entire sky all of the time. This allowed us to observe unpredictable events such as black hole state changes in Cyg X-1, 1E 1740-29, GX 339-4, and Cyg X-3 (Harmon et al. 2004 and references therein) and to find pre-discovery emission in archival data. We discovered extremely bright flares, shown in Figures 3 and 4, from GRS 1915+105 from data prior to its discovery (Paciasas et al. 1996). In addition, BATSE data were very useful for studying long-term trends in source behaviors and were important components in several multiwavelength campaigns (e.g. Cyg X-3, McCollough et al 1999). With the BATSE Earth occultation technique, we discovered three new black hole transient systems, GRO J0422+32, GRO J1655-40, and GRO J1719-24=GRS 1716-249.

### 3.2. GBM

We have a guest investigation program (P.I. Wilson-Hodge) in place to implement the Earth occultation technique with GBM. Implementation of the technique is in progress. For GBM, the technique is complicated by the fact that Fermi is scanning the sky, rather than being interially pointed like CGRO. This means the detector response is changing and must be taken into account. Figure 5 shows a rising Earth occultation step from Sco X-1 in GBM NaI #2. Figure 6 shows the estimated GBM sensitivity taking into account the expected backgrounds, which are consistent with observed rates. GBM

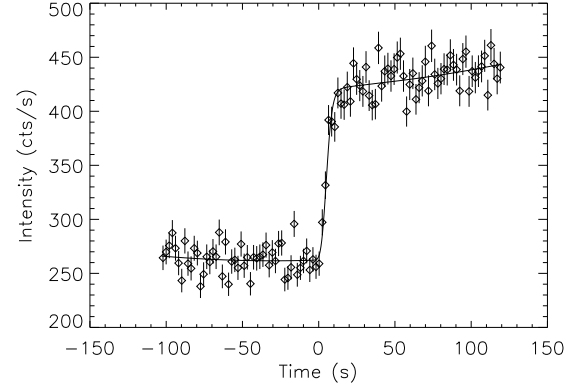


Fig. 5. An example Earth occultation step observed with GBM on 2008 September 21 from Sco X-1 in the 10-25 keV band. The diamonds denote the raw CTIME count rates measured with GBM plotted at 2 s resolution. The solid line denotes the fitting model which consists of a quadratic background plus an atmospheric transmission function convolved with predicted count rates for Sco X-1. The predicted count rates result from folding an assumed spectral model through the changing detector response function as the spacecraft moves.

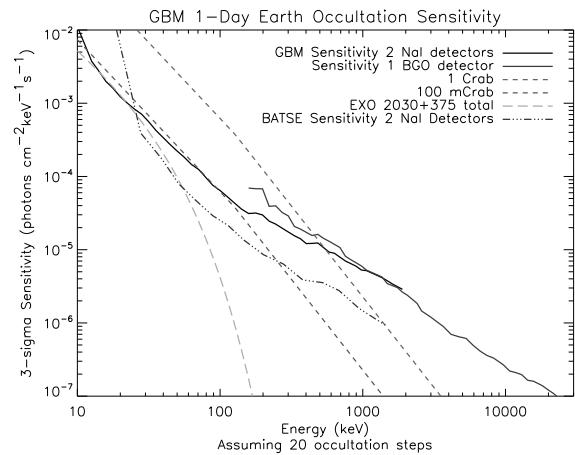


Fig. 6. The estimated 1-day Earth occultation sensitivity limits for two GBM NaI detectors and one GBM BGO detector for a source at moderate viewing angles. The BATSE sensitivity limit for 2 LADs is shown for comparison. Also shown are 1 Crab and 100mCrab spectra, as well as the spectrum of the accreting X-ray pulsar EXO 2030+375.

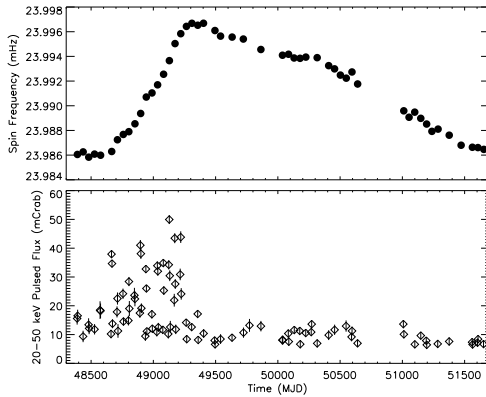


Fig. 7. (*top*): Barycentered, orbit corrected spin-frequency for EXO 2030+375 at each periastron passage where BATSE detected pulsations. (*bottom*): Corresponding 20-50 keV pulsed flux for these observations measured with BATSE.

has considerably better sensitivity from about 8-25 keV than BATSE because the GBM NaI detectors have only a Be window instead of the plastic scintillator, aluminum honeycomb, and aluminum window located in front of the BATSE detectors. The 1-day sensitivity limit for the Earth occultation technique with GBM assuming a source is viewed by two NaI detectors is about 90 mCrab below 100 keV (Case et al. 2007). The Japanese Monitor of All-Sky X-ray Image (MAXI), described in detail elsewhere in these proceedings and scheduled to be attached to the space station in 2009, has much better sensitivity, but only extends up to 30 keV. Earth occultation monitoring with GBM will provide the only all-sky capability above about 50 keV. Hence GBM will provide important complementary data for bright events observed with MAXI.

### 3.3. Accreting Pulsar Observations

Accreting X-ray pulsars consist of a magnetized neutron star ( $B \sim 10^{12}$  G) orbiting a companion. Accretion in these systems occurs via either Roche lobe overflow, a stellar wind, or interaction with the circumstellar disk of a Be star near periastron passage. Recently, *INTEGRAL* has discovered a number of likely highly absorbed wind accreting X-ray pulsars (Walter et al. 2006).

### 3.4. BATSE

A large number of accreting pulsars were monitored daily with BATSE. For example, Figure 7 shows the spin-frequency history and the pulsed flux measured for the accreting Be/X-ray pulsar EXO 2030+375. Each point corresponds to a periastron passage in the system, when the source was typically detectable for 4-12 days. Monitoring of this particular pulsar led to the discovery that the infrared magnitudes showed a decline shortly before the pulsar began to spin down and the pulsed

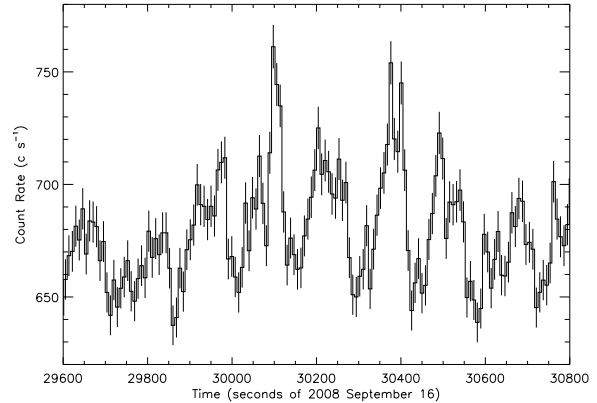


Fig. 8. An example of an accreting X-ray pulsar in the GBM data. This Figure shows 283-s pulses from Vela X-1 in the 12-52 keV energy band for GBM NaI 4.

flux abruptly dropped (Wilson et al. 2002). This implied that the density of the disk around the companion star declined, making less material available for accretion onto the pulsar. Later, after CGRO deorbited, the infrared magnitudes again brightened accompanied by a brightening of the X-ray outbursts and a transition to spin-up observed with the Rossi X-ray Timing Explorer (Wilson et al 2005).

The techniques used to detect known accreting pulsars with BATSE are described in detail elsewhere (Bildsten et al. 1997, Finger et al. 1999). The basic idea is that the data, when the pulsar of interest was above the horizon, were fitted with a model consisting of a background plus a Fourier expansion in the pulse phase model which used an approximately known spin-frequency. This model was used to generate pulse profiles for short segments of data, short enough that the loss of power due to phase drift was small. These short segment profiles were then shifted using a grid in pulse frequency and sometimes frequency derivative. The shifted profiles were combined and the best frequency (and derivative) was selected from the grid using a modified  $Z_n^2$  statistic. In addition to this technique, daily fast Fourier transforms of the BATSE data were performed to look for new periodicities in the data. Six new accreting pulsars were discovered with BATSE: GRO J1008-57, GRO J1948+32, GRO J1744-29, GRO J2058+42, GRO J1750-27, and GRO J1944+26 = XTE J1946+274.

### 3.5. GBM

We have a guest investigation program in place to monitor accreting pulsars using GBM (PI Finger). We expect that GBM should be able to detect most of the X-ray pulsars observed with BATSE, despite GBMs smaller area. This is because of the fortunate combination of a large number of photons in the 8-25 keV range from

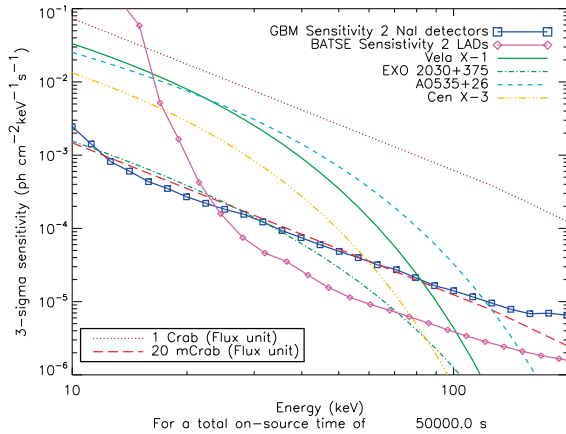


Fig. 9. Estimated GBM 3- $\sigma$  root-mean squared (rms) pulsed flux sensitivity to accreting X-ray pulsars for 50 ks on-source. For comparison, we show BATSE's sensitivity and representative rms pulsed flux spectra for the accreting X-ray pulsars Vela X-1, EXO 2030+375, A 0535+262, and Cen X-3. One Crab and 20 mCrab flux units are also shown for reference.

most accreting pulsars combined with GBMs improved low-energy response over BATSE. For accreting pulsars, GBM will provide daily monitoring of spin-frequencies, while MAXI will provide precise flux measurements. Together these results will be excellent for studying correlations between pulsar spin-up rates and total flux. Figure 8 shows pulses from the 283-s wind-fed accreting X-ray pulsar, Vela X-1, that are visible in the raw data.

Figure 9 shows the result of our sensitivity calculation in terms of rms pulsed flux. Details of the calculation are given in Wilson-Hodge et al. (2007). For reference, we have also done the same calculation for the BATSE LADs using actual measured background rates and corresponding detector response matrices for two detectors. Typical rms pulsed flux spectra of 4 accreting pulsars are also shown that were detectable with BATSE and are expected to be detectable with GBM.

#### 4. Conclusions

BATSE observed 2704 triggered GRBs and provided the first clear evidence that GRBs were cosmological. With BATSE, we monitored the sky using Earth occultation measurements in the 20-1800 keV band, providing important contributions to multiwavelength studies, long-term studies, and observations of unpredictable events such as state changes in black holes. We provided the only continuous monitoring of accreting pulsar spin-frequencies, including transitions from spin-up to spin-down. Most BATSE data are still available through NASA's High Energy Astrophysics Science Archive Research Center (<http://heasarc.gsfc.nasa.gov>) for archival studies.

Using GBM we will continue all-sky monitoring observations. It is still very early in the mission, but results so far look exciting. GBMs most important contributions will most likely be for GRBs where, combined with the LAT, we will provide the broadest spectral coverage ever achieved. Plus we will complement GRB observations from other instruments, such as Swift, providing higher energy coverage with our BGO detectors. Today, other all-sky monitors are also available such as the Burst Alert Telescope on-board Swift (15-150 keV, Barthelmy et al. 2005) and in 2009, MAXI (0.5-30 keV). GBM data will complement these other monitors, providing additional time coverage in the 8-50 keV band, the only high energy source monitoring above about 50 keV, and the only near-continuous monitoring of accreting pulsar spin-frequencies.

#### References

- Barthelmy, S.D. et al. 2005, *Space Science Reviews*, 120, 143
- Bildsten, L. et al. 1997, *ApJS*, 113, 367
- Case, G.L. et al. 2007, *The First GLAST Symposium*, AIP Conf. Proc. 921, eds. S.Ritz, P. Michelson, C. Meegan, (AIP: Melville), 538
- Finger, M.H., et al. 1999, *ApJ*, 517, 449
- Harmon et al. 2004, *ApJS*, 154, 585
- McCollough, M.L. et al. 1999, *ApJ*, 517, 951
- Meegan, C.A. et al. 2007, *The First GLAST Symposium*, AIP Conf. Proc. 921, eds. S.Ritz, P. Michelson, C. Meegan, (AIP: Melville), 13
- Paciesas, W.S. et al. 1996, *A&AS*, 120, 205
- Paciesas, W.S. et al. 1999, *ApJS*, 122, 465
- Walter, R. et al. 2006, *A&A*, 453, 133
- Wilson, C.A. et al 2002, *ApJ*, 570, 287
- Wilson, C.A., Fabregat, J., Coburn, W. 2005, *ApJ*, 620, L99
- Wilson-Hodge, C.A. et al. 2007, *The First GLAST Symposium*, AIP Conf. Proc. 921, eds. S.Ritz, P. Michelson, C. Meegan, (AIP: Melville), 229